JOURNAL OF ELECTROMAGNETIC ENGINEERING AND SCIENCE, VOL. 15, NO. 3, 185~193, JUL. 2015

http://dx.doi.org/10.5515/JKIEES.2015.15.3.185
ISSN 2234-8395 (Online) · ISSN 2234-8409 (Print)

Hybrid MIMO Antenna Using Interconnection Tie for Eight-Band Mobile Handsets

Wonhee Lee · Mingil Park · Taeho Son*

Abstract

In this paper, a hybrid multiple input multiple output (MIMO) antenna for eight-band mobile handsets is designed and implemented. For the MIMO antenna, two hybrid antennas are laid symmetrically and connected by an interconnection tie, thereby enabling complementary operation. The tie affects both the impedance and radiation characteristics of each antenna. Further, printed circuit board (PCB) embedded type is applied to the antenna design. To verify the results of this study, we designed eight bands-LTE class 12, 13, and 14, CDMA, GSM900, DCS1800, PCS, and WCDMA-and implemented them on a bare board the same size as the real board of a handset. The voltage standing wave ratio (VSWR) is within 3:1 over the entire design band. Antenna isolation is less than −15 dB at the lower band, and −12 dB at the WCDMA band. Envelope correlation coefficient (ECC) of 0.0002–0.05 is obtained for all bands. The average gain and efficiency are measured to range from −4.69 dBi to −2.88 dBi and 33.99% to 51.5% for antenna 1, and −4.74 dBi to −2.97 dBi and 33.45% to 50.49% for antenna 2, respectively.

Key Words: Hybrid Antenna, Internal Antenna, LTE, MIMO, Mobile Handset Antenna.

I. INTRODUCTION

Long Term Evolution (LTE) has become a popular standard in mobile communication techniques. In LTE, new channels have been recently allocated to low LTE bands, including class 12 (698–746 MHz), class 13 (746–787 MHz), class 14 (758–798 MHz), class 17 (704–746 MHz), class 5 (824–894 MHz), class 6 (830–885 MHz), and class 8 (880–960 MHz). Due to these low LTE channels, mobile handset antennas must cover a range of 698–960 MHz. Hence, mobile handsets must utilize wide-band antennas that can cover all the voice communication bands, including the allocated low LTE bands [1]. This is a current issue for antenna techniques. Recently, the inverted F antenna (IFA) has been widely used as an internal antenna in mobile handsets. Owing to the space limitations in the handset, it is rather challenging for IFA to achieve wideband operation. Moreover, modern antennas need to be prepared to cover all service bands (698–960 MHz and 1,710–2,170 MHz), including LTE class 12–14 for the low bands of LTE application. Another issue is the MIMO system. High-rate data communication must provide reliable transfer rates and high transmission speed. The MIMO antenna should meet these requirements. Therefore, the MIMO antenna must have a low envelope correlation coefficient (ECC) from the high isolation between antennas. The design target of the MIMO antenna is determining how to obtain a high isolation performance and low ECC for high diversity gain. Antennas for high frequency mobile band can be easily developed, because of the short wavelength. However, it is difficult to build antennas for low frequency bands, such as

Manuscript received March 12, 2015 ; Revised June 10, 2015 ; Accepted June 10, 2015. (ID No. 20150312-013J)
Department of IT Engineering, Soonchunhyang University, Asan, Korea.
*Corresponding Author: Taeho Son (e-mail: thson@sch.ac.kr)

LTE700 (classes 12–14) and CDMA, within the limited space of a mobile handset. Moreover, long wavelengths in small spaces leads to weak isolation of the MIMO antenna, due to mutual coupling between antennas.

Many studies have attempted to design antennas related to wideband application [2–6], but few have discussed wideband MIMO antennas. All band antennas have been proposed through the closely coupled parasitic structure [2] and the hybrid antenna using the coupled feeding structure [5, 6]. These studies achieved wide and multi bandwidth, but not in the case of the MIMO antenna. Another study using a split ring resonator and T-shape isolator were presented for improving the isolation of the MIMO antenna. However, these are only for high mobile frequency bands [7, 8]. While a four-port MIMO antenna was studied for the 700 MHz and 2,400 MHz dual-band MIMO system [9], it did not include other bands such as CDMA, GSM, DCS, PCS and WCDMA. In addition, an antenna using resonance of ground plane was proposed for wideband MIMO antenna [10]. However, it not only had a complicated structure, but also did not include the GSM band.

In this study, a wideband antenna with low ECC MIMO was designed and implemented. Two hybrid antennas were symmetrically laid and connected by an interconnection tie. A hybrid antenna comprising a monopole antenna and an IFA was employed to achieve wide bandwidth. Two hybrid antennas operated in complement to each other via the interconnection tie, which affected both the characteristics of antenna impedance and radiation efficiency. The interconnection tie was shown to improve performances of both return loss and isolation between antennas. Variances of return loss, according to a change in variable antenna lengths and locations of interconnection tie, were simulated for optimum design. A PCB embedded MIMO antenna for LTE classes 12 (698–746 MHz), 13 (746–787 MHz), and 14 (758–798 MHz); CDMA (824–896 MHz); GSM900 (880–960 MHz); DCS1800 (1,710–1,880 MHz); PCS (1,750–1,910 MHz); and WCDMA (1,920–2,170 MHz) was designed and implemented on a 60 mm × 115 mm FR4 PCB. The return losses and radiation characteristics of the implemented antenna were also measured. The remainder of the paper is organized in the following manner: Section II describes the principles of the antenna design, Section III compares the measurement results with simulations, and Section IV concludes the paper.

II. Hybrid MIMO Antenna Design

The proposed MIMO antenna was based on monopole and IFA hybrid antennas. Two hybrid antennas were laid symmetrically and connected by an interconnection tie. The antenna

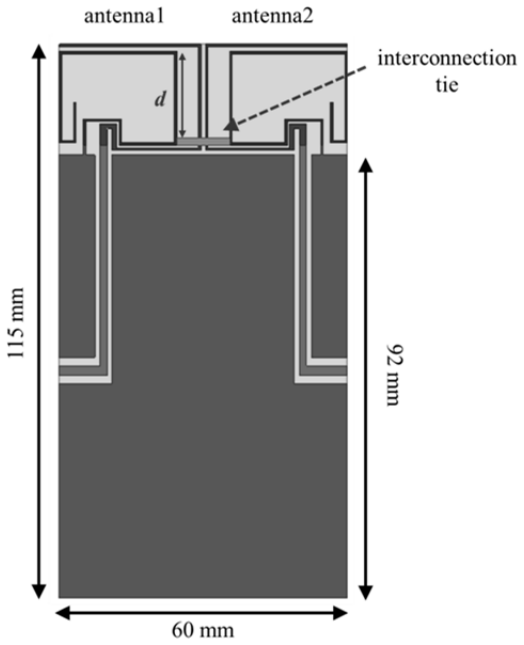

Fig. 1. Geometry of the proposed antenna.

was designed on a bare board in the geometry depicted in Fig. 1, and implemented on a PCB of 60 mm × 115 mm FR4 substrate of relative dielectric constant $\varepsilon_r = 4.4$ with a thickness of $h = 1.0$ mm. The PCB ground size was 60 mm × 92 mm. Details regarding the geometry parameters of the hybrid MIMO antenna are presented in Fig. 2. All units are given in millimeters. The interconnection tie was 10 mm long, and it connected the two antennas as a bridge that was 1 mm high and 1.5 mm wide.

Fig. 3 illustrates the structure of an element antenna of the

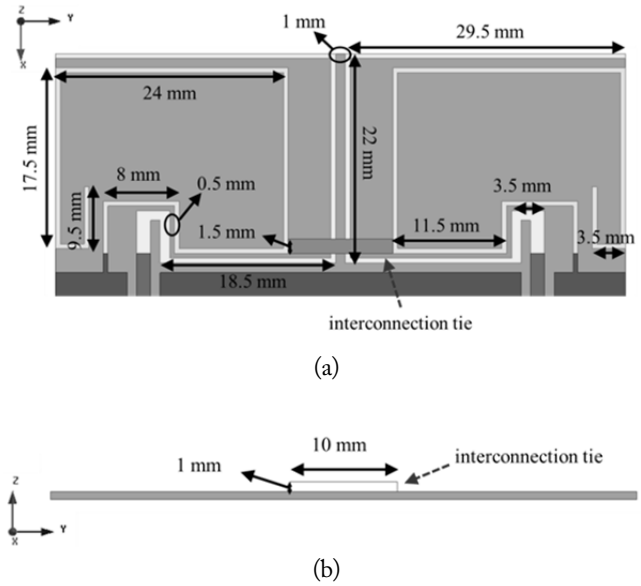

Fig. 2. Detailed geometry of the interconnection tie for the multiple input multiple output (MIMO) antenna: (a) x-y plane and (b) y-z plane.

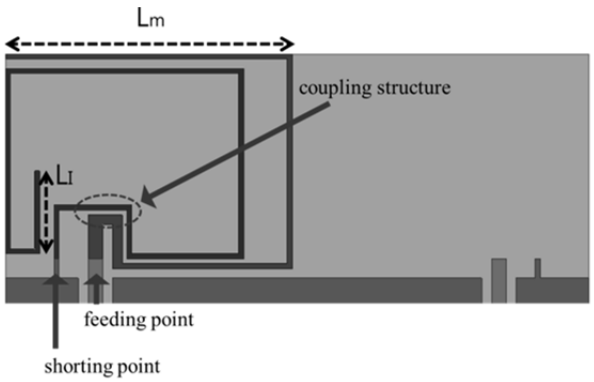

Fig. 3. Structure of an element antenna.

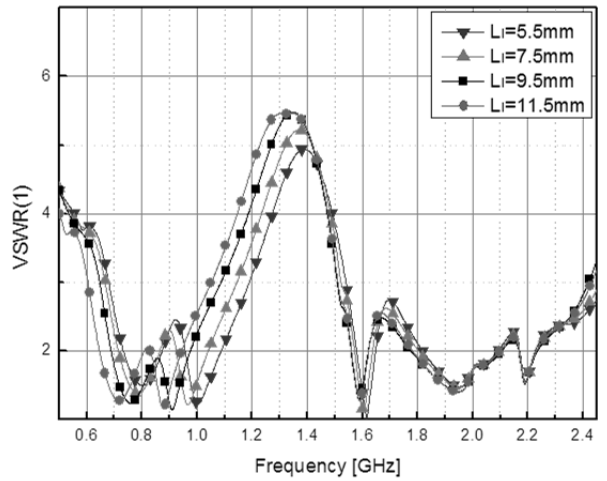

(a)

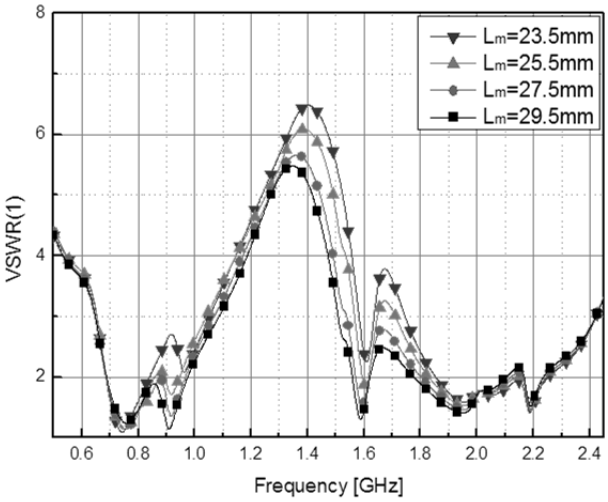

(b)

Fig. 4. Simulated voltage standing wave ratio (VSWR) of the element antenna as a function of (a) the inverted F antenna length L_I and (b) the monopole length L_m in Fig. 3.

proposed antenna. The element antenna comprises a monopole and an IFA. The system feeder basically fed the monopole antenna, while the IFA was fed by the coupled current fed from the monopole. Therefore, the element antenna simultaneously operates a monopole antenna and an IFA. The resonant frequencies of the two antennas were combined, thereby enabling the hybrid antenna to serve wider bands. In this study, the hybrid antenna was used to satisfy the wide bandwidths of eight bands (LTE classes 12, 13, and 14; CDMA; and GSM for the lower band, and DCS, PCS, and WCDMA for the upper band). Generally, the length of the IFA is longer than the monopole antenna at the lower frequency band. Therefore, the IFA was designed to operate for LTE class 13. Further, the monopole antenna was designed to operate for the CDMA and GSM900 bands. Fig. 4 illustrates the simulated VSWR of the element antenna as a function of the IFA length L_I (a) and the monopole length L_m in Fig. 3. When the lengths L_I and L_m are longer, the resonant frequencies move toward a low frequency.

Consequently, the VSWR of the element antenna was satisfied within 3:1 for all mobile service bands, as shown in Fig. 5. The EM simulation for the antenna design was conducted using Ansoft HFSS version 13.

The general MIMO antenna, depicted in Fig. 6, has problems related to mutual coupling due to the insufficient gap between antennas. Thus, the antenna operation is more capacitive than inductive. Consequently, the resonance frequency is shifted higher, or the resonance does not sufficiently occur. This problem can be solved by the interconnection tie, which can contribute to high isolation through the reduction of mutual coupling.

The simulated electric field density (V/m) of the hybrid MIMO antenna is presented in Fig. 7. Fig. 7(a) depicts the results of an MIMO antenna without an interconnection tie, while Fig. 7(b) illustrates the result of the proposed MIMO antenna with an interconnection tie at the frequency of 698 MHz. The frequency of 698 MHz was chosen because it is the lowest frequency.

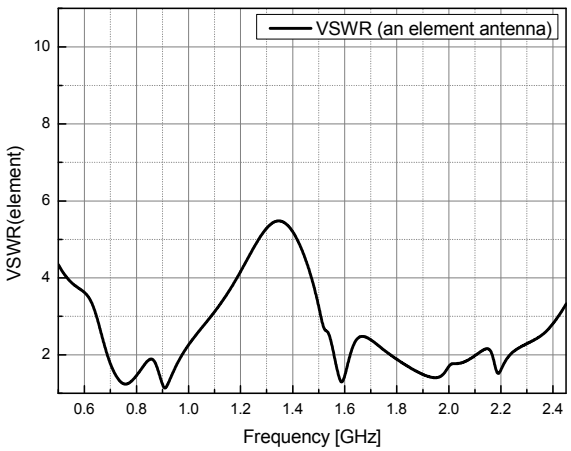

Fig. 5. Simulated voltage standing wave ratio (VSWR) of the element antenna.

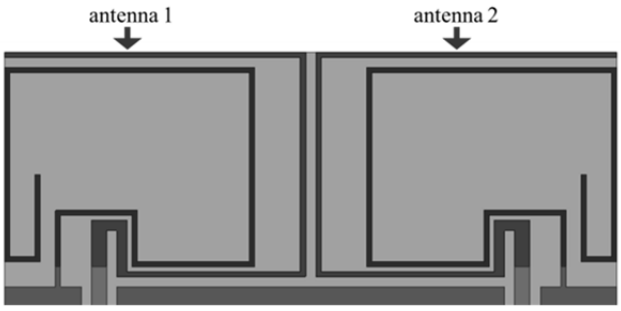

Fig. 6. Multiple input multiple output (MIMO) antenna without an interconnection tie.

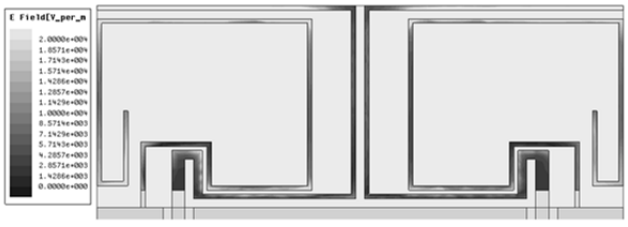

(a)

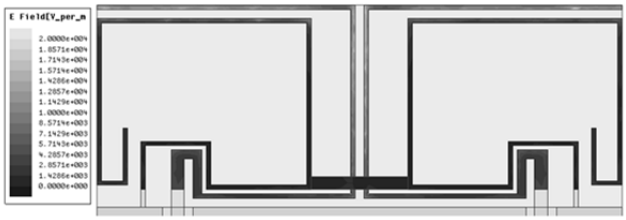

(b)

Fig. 7. Comparison of simulated electric field strength of (a) multiple input multiple output (MIMO) antenna without an interconnection tie, and (b) the proposed MIMO antenna with an interconnection tie at 698 MHz.

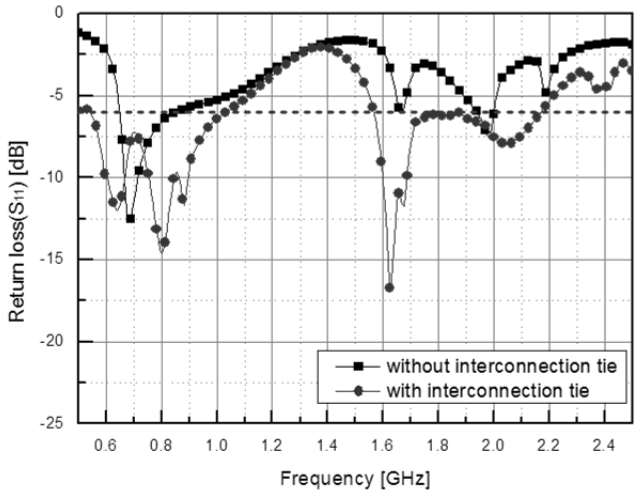

(a)

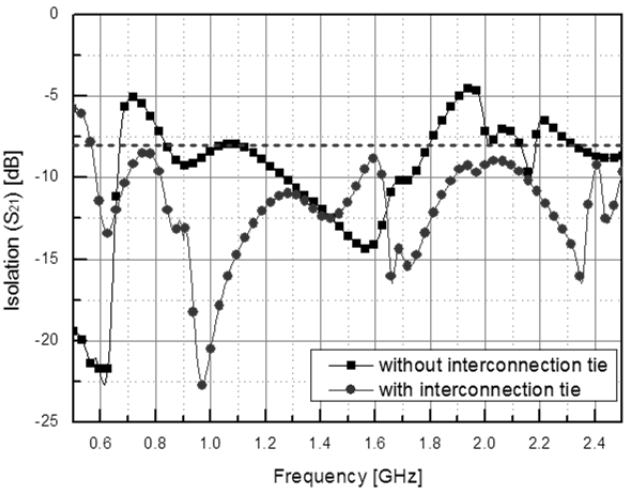

(b)

Fig. 8. Comparison of simulated (a) return loss (S_{11}) and (b) isolation between the multiple input multiple output (MIMO) antenna without an interconnection tie and the proposed antenna.

The lowest frequency is the most severe when considering mutual coupling between two antennas. As observed in Fig. 7, the electric field strength of the proposed antenna with an interconnection tie was reduced compared to that of the antenna without an interconnection tie. Note that the interconnection tie caused a reduction of the mutual coupling between the antennas.

Fig. 8 presents a comparison of return loss and isolation between the proposed antenna with an interconnection tie and the MIMO antenna without the tie. The two tested antennas had the same dimensions in order to allow isolation of the effect of the interconnection tie. As shown in Fig. 8(a), return loss with no interconnection was worse than that of the element antenna presented in Fig. 5. This problem was caused by the mutual coupling between antennas. Therefore, the MIMO antenna without an interconnection tie showed narrow bandwidths in the lower band, and poor impedance performance in the upper band. In contrast, the proposed antenna with interconnection tie showed better performance in both the lower and upper bands, because the mutual coupling was reduced by the interconnection tie. The isolation between antennas is illustrated in Fig. 8(b). The proposed antenna displayed better isolation than that without an interconnection tie. These results indicate that the monopole and IFA of the proposed antenna operated normally via the inter-connection tie, as indicated in Fig. 7.

For optimum design of the interconnection tie, VSWR and isolation (S_{21}), as functions of the tie position d in Fig. 1, were simulated as shown in Fig. 9. Tie position d was varied from 12 mm to 18 mm, in 2 mm steps. The tie position affected the VSWR in Fig. 9(a) and isolation in Fig. 9(b) more in the upper band than in the lower band. This implies that tie position did not influence the lower band, but had an effect on

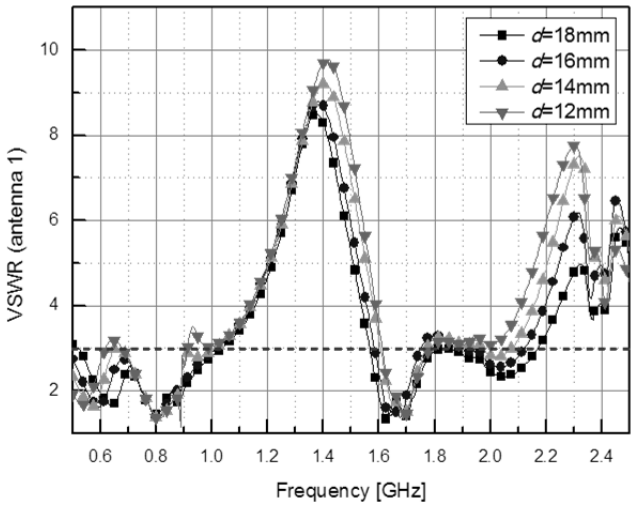

(a)

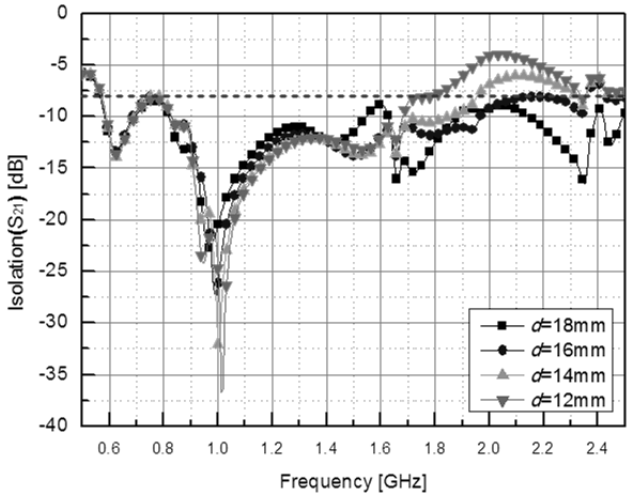

(b)

Fig. 9. Comparison of simulated (a) voltage standing wave ratio (VSWR) and (b) isolation as a function of the interconnection tie position *d* in Fig. 1.

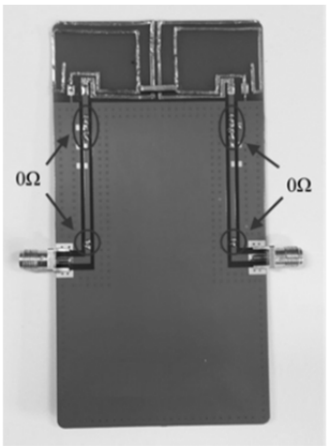

Fig. 10. Proposed multiple input multiple output (MIMO) antenna implemented on a printed circuit board.

the upper band. The *d* of 18 mm was found to be the best position, as shown in Fig. 9.

III. Results and Discussion

The proposed MIMO antenna, illustrated in Fig. 10, was implemented and measured experimentally. The dimensions of the antenna and PCB are as depicted in Figs. 1 and 2. Two SMA connectors were used at the feeding port of the coplaner waveguide with a ground (CPWG) feed line. The *S*-parameter was measured using the Agilent-E5062A two-port network analyzer, and the antenna radiation patterns were measured in an anechoic chamber.

The results of the simulated and measured return losses of the proposed antenna are depicted in Fig. 11. The simulated and measured return loss of the proposed antennas satisfied the return loss of under −6 dB, which is within the VSWR 3:1. For antenna 1, illustrated in Fig. 11(a), the simulated −6 dB

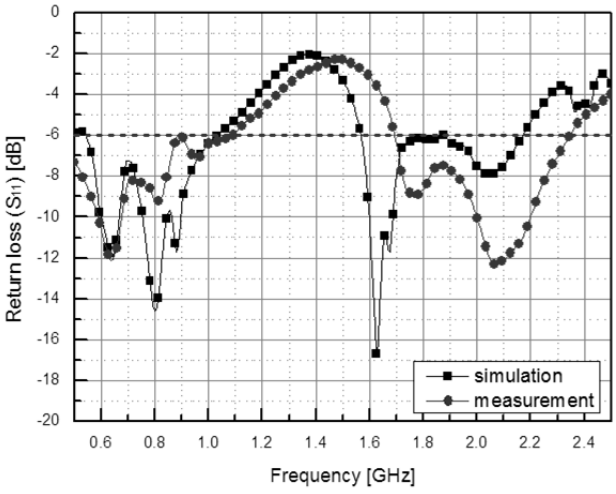

(a)

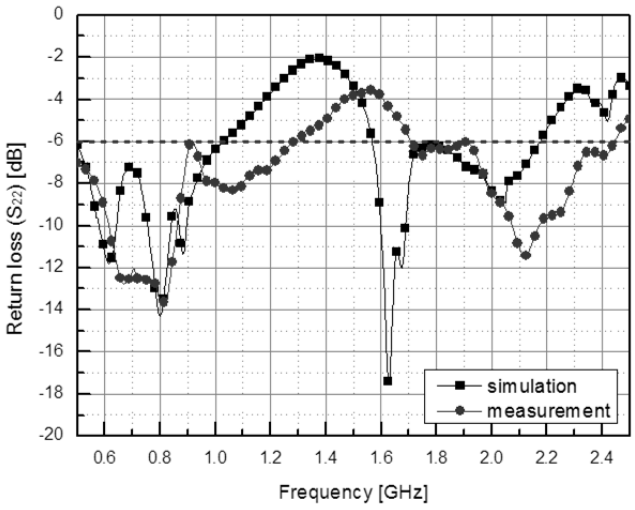

(b)

Fig. 11. A comparison of simulated and measured return loss of (a) antenna 1 and (b) antenna 2.

bandwidth showed a range of 520 MHz (500–1,020 MHz) or 68.42% bandwidth for the lower band, and 610 MHz (1,560–2,170 MHz) or 32.7% bandwidth for the upper band. The lower bandwidth measured for antenna 1 showed a range of 590 MHz (500–1,090 MHz) or 74.21%, thereby satisfying the requirements for LTE700 (classes 13 and 14), CDMA, and GSM900 bands, while the upper bandwidth showed bandwidths of 640 MHz (1,700–2,340 MHz) or 31.68%, covering the mobile service bands of DCS, PCS, and WCDMA. For antenna 2 in Fig. 11(b), the simulated and measured bandwidth data showed a wide band-width, like antenna 1 in Fig. 11(a). Generally, the measured data agreed well with the simulation results. However, the measurement frequencies shifted a little higher than the simulation frequencies. The main reason for this is probably the different environments of the ground condition, as well as implementation errors between simulation and measurement.

The simulated and measured isolations are presented in Fig. 12. The specification for the isolation between antennas for the MIMO communication is less than −8 dB. The proposed antenna satisfied the isolation specifications in both the simulation and measurement over the entire design band. The maximum measured isolation for LTE700, CDMA, and GSM900 bands was −15 dB, and for DCS to WCDMA bands was −10 dB. Thus, the simulated isolation of the proposed antenna agreed comparatively well with the measurements.

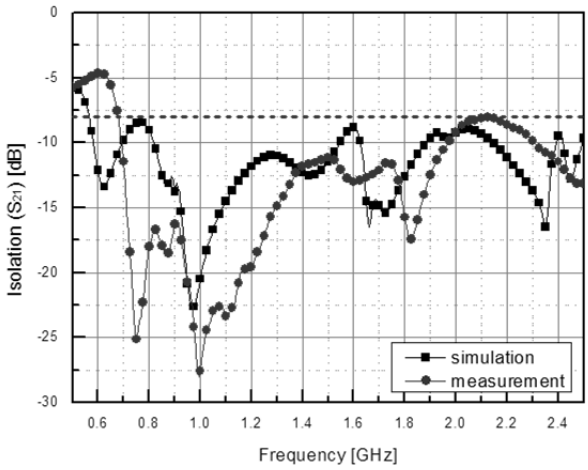

Fig. 12. A comparison of simulated and measured isolation of antenna.

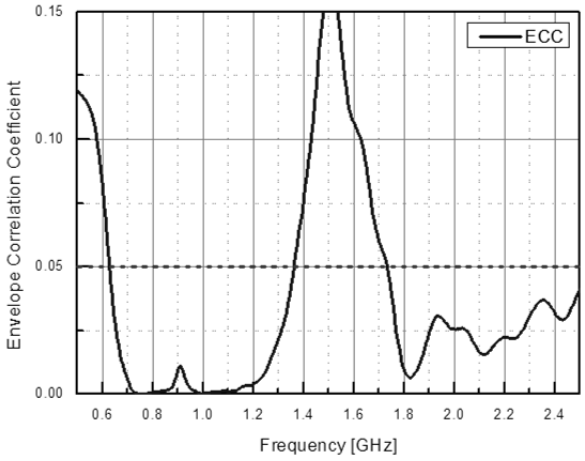

Fig. 13. Envelope correlation coefficient of antenna.

The ECC is used to evaluate the diversity capability factor of MIMO antenna systems [11, 12]. The ECC ρ_e calculated from the *S*-parameters can be obtained using Eq. (1).

$$\rho_e = \frac{|S_{11}{}^{*}S_{12}+S_{12}{}^{*}S_{22}|^2}{(1-(|S_{11}|^2+|S_{21}|^2))(1-(|S_{22}|^2+|S_{12}|^2))} \quad (1)$$

From the measured *S*-parameter data of the antenna, the ECC ρ_e was computed and is depicted in Fig. 13. At the LTE700 band (classes 13 and 14), the maximum ECC ρ_e obtained was 0.0002, which is very small. In addition, the ECC for the CDMA and GSM900 bands varied from 0.001 to 0.009, while the upper bands of DCS, PCS, and WCDMA ranged from 0.006 to 0.05.

The ECC must be below 0.5 for MIMO system performance [13, 14]. Therefore, the ECC obtained for the proposed antenna is promising for MIMO antenna operation.

Fig. 14 illustrates the H-plane patterns of the proposed antenna. The omnidirectional radiation pattern at the H-plane was observed in the lower band, as depicted in Fig. 14(a). The radiation patterns for the upper band in Fig. 14(b) displayed more variation, but no nulls. Note that the H-plane radiation patterns of the internal antenna are generally dependent on the ground size of the mobile phone, particularly for frequencies in the upper band. The wavelength of the upper band is shorter than the length of the phone ground. This generates the variations and nulls in the radiation patterns.

Nevertheless, the measured H-plane radiation patterns for the proposed antenna showed almost omnidirectional characteristics. The measured co- and cross-polarization radiation patterns of antenna at the same frequency band as that in Fig. 14 are presented in Fig. 15.

Fig. 16 illustrates the measured 3-dimensional radiation patterns at 720, 960, 1,820, and 2,170 MHz for free space. The antenna was tested in a far-field anechoic chamber, the MTG model. All patterns showed stable radiation patterns, and the proposed antenna had good radiation patterns for the mobile communication handset. However, null was observed in the radiation pattern at 2,170 MHz. The measured antenna average gains and efficiencies over eight band frequencies are summarized in Table 1. The average gains and efficiencies for the lower band of antenna 1 were measured as −4.69 to −3.21 dBi and 33.99% to 47.77%, respectively. The average gains

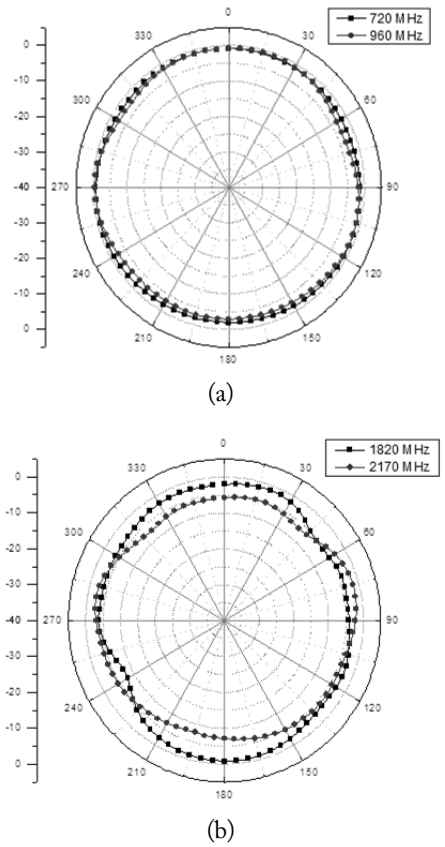

Fig. 14. Measured (a) lower band and (b) upper band H-plane patterns of antenna.

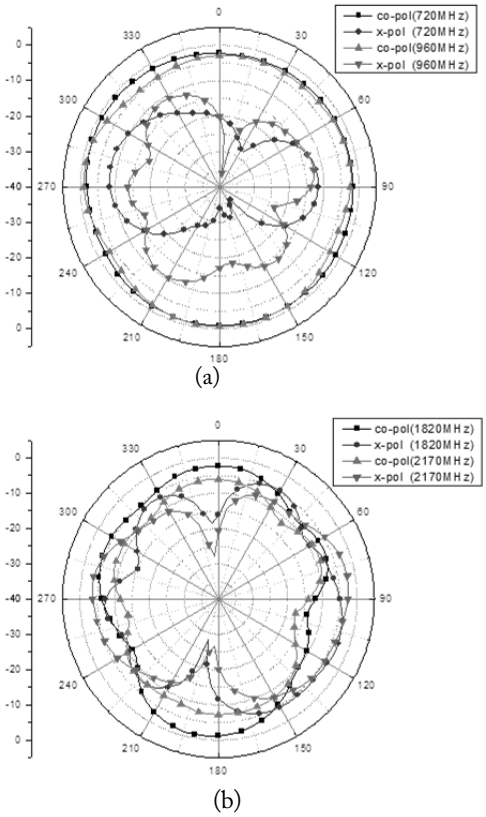

Fig. 15. Measured co- and cross-polarization radiation patterns of antenna at (a) 720 MHz and 960 MHz, (b) 1,820 MHz and 2,170 MHz (y-z plane, θ = 90°).

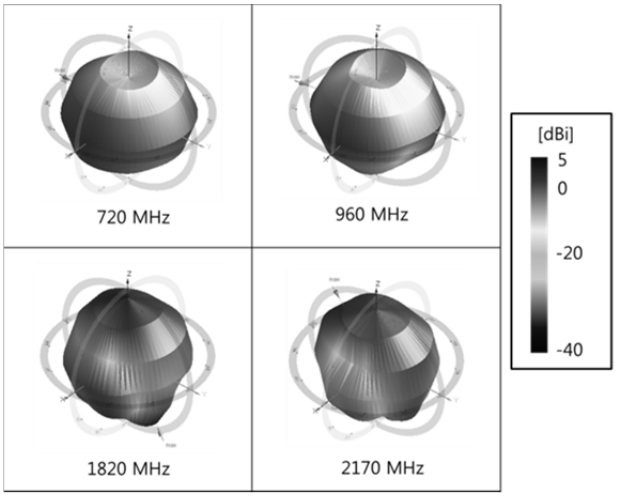

Fig. 16. Measured 3-dimensional radiation patterns of antenna.

Table 1. Measured antenna average gains and efficiencies

Freq.	Antenna 1		Antenna 2	
(MHz)	Eff. (%)	Avg. (dBi)	Eff. (%)	Avg. (dBi)
698	39.36	−4.05	36.55	−4.37
710	41.04	−3.87	38.94	−4.10
750	47.77	−3.21	45.13	−3.46
824	45.20	−3.45	40.73	−3.90
849	43.76	−3.59	42.21	−3.75
869	41.94	−3.77	34.44	−4.63
894	34.88	−4.57	33.45	−4.74
910	33.99	−4.69	41.45	−3.83
930	41.82	−3.79	41.35	−3.84
960	41.82	−3.79	45.71	−3.40
1,710	46.51	−3.32	35.77	−4.46
1,770	36.89	−4.33	50.49	−2.97
1,820	51.50	−2.88	43.34	−3.64
1,850	45.00	−3.47	36.83	−4.34
1,880	39.35	−4.05	45.42	−4.51
1,910	38.67	−4.13	36.48	−4.38
1,930	39.38	−4.05	33.66	−4.73
2,170	35.91	−4.45	38.34	−4.16

and efficiencies for the lower band of antenna 2 were −4.74 to −3.40 dBi and 33.45% to 45.71%, respectively. The average gains and efficiencies for the upper band of antenna 1 were measured to be −4.45 to −2.88 dBi and 35.91% to 51.50%, with −4.73 to −2.97 dBi and 33.66% to 50.49% for antenna 2, respectively. The measured results indicated that the performances in terms of bandwidth, gain, and efficiency of the proposed MIMO antenna were met or were better than those of the recent MIMO antenna.

IV. Conclusion

In this study, a mobile phone MIMO antenna using an interconnection tie for eight-band mobile communication

services was proposed. It was shown that the mutual coupling between antennas can be reduced by the application of the interconnection tie, and the proposed MIMO antenna achieved better characteristics for both bandwidth and isolation. The antenna was implemented and tested herein. The wide operating band, covering 700–1,400 MHz and 1,700–2,200 MHz, was obtained within VSWR 3:1. The application of an interconnection tie enabled reduction of the maximum isolation to −12 dB from −6 dB. In addition, omnidirectional H-plane radiation patterns were observed at the operating bands. The ECC of the proposed MIMO antenna displayed good characteristics, thereby obtaining less than 0.0002 for the LTE700 band, between 0.001 and 0.05 for the CDMA and GSM900 band, and below 0.05 for the WCDMA band. Average gain and efficiency were determined to be from −4.69 to −2.88 dBi and 33.99% to 51.5% for antenna 1, and −4.74 to −2.97 dBi and 33.45% to 50.49% for antenna 2, respectively. The proposed antenna can be implemented easily and has a low cost of application to mobile phones. This study is expected to promote the research and applications for mobile communication MIMO antennas to multiple mobile services, including the LTE700 band.

This research was supported by the Basic Science Research Program through the National Research Foundation of Korea funded by the Ministry of Education (No. 2015-023260).

REFERENCES

[1] S. Zhang, A. A. Glazunov, Z. Ying, and S. He, "Reduction of the envelope correlation coefficient with improved total efficiency for mobile LTE MIMO antenna arrays: mutual scattering mode," *IEEE Transactions on Antennas and Propagation*, vol. 61, no. 6, pp. 3280−3291, 2013.

[2] F. H. Chu and K. L. Wong, "Planar printed strip monopole with a closely-coupled parasitic shorted strip for eight-band LTE/GSM/UMTS mobile phone," *IEEE Transactions on Antennas and Propagation*, vol. 58, no. 10, pp. 3426−3431, 2010.

[3] S. C. Chen and K. L. Wong, "Bandwidth enhancement of coupled fed on-board printed PIFA using bypass radiating strip for eight-band LTE/GSM/UMTS slim mobile phone," *Microwave and Optical Technology Letters*, vol. 52, no. 9, pp. 2059−2065, 2010.

[4] K. L. Wong, M. F. Tu, T. Y. Wu, and W. Y. Li, "Small-size coupled-fed printed PIFA for internal eight-band LTE/GSM/UMTS mobile phone antenna," *Microwave and Optical Technology Letters*, vol. 52, no. 9, pp. 2123−2128, 2010.

[5] S. J. Lim and T. H. Son, "Hybrid antenna for the all band mobile phone service including LTE," *Journal of Korean Institute of Electromagnetic Engineering and Science*, vol. 22, no. 7, pp. 737−743, 2011.

[6] M. K. Chun and T. H. Son, "PIFA and IFA hybrid antenna for the data communication terminal," *Journal of the Korea Institute of Intelligent Transport Systems*, vol. 10, no. 4, pp. 65−70, 2011.

[7] G. Kim and B. Lee, "Metamaterial-based zeroth-order resonant antennas for MIMO applications," *Journal of Electromagnetic Engineering and Science*, vol. 13, no. 3, pp. 195−197, 2013.

[8] Y. Lee, H. Chung, and J. Choi, "Improving the isolation of MIMO antennas using split ring resonators," *Journal of Electromagnetic Engineering and Science*, vol. 10, no. 4, pp. 303−308, 2010.

[9] Y. C. Lu, Y. C. Chan, H. J. Li, and Y. C. Lin, "Design and system performances of a dual-band 4-port MIMO antenna for LTE applications," in *Proceedings of IEEE International Symposium on Antennas and Propagation (APSURSI)*, Spokane, WA, 2011, pp. 2227−2230.

[10] X. Zhao, K. Kwon, and J. Choi, "MIMO antenna using resonance of ground planes for 4G mobile application," *Journal of Electromagnetic Engineering and Science*, vol. 13, no. 1, pp. 51−53, 2013.

[11] S. Blanch, J. Romeu, and I. Corbella, "Exact representtation of antenna system diversity performance from input parameters description," *Electronics Letters*, vol. 39, no. 9, pp. 705−707, 2003.

[12] T. W. Kang, K. L. Wong, and M. F. Tu, "Internal handset antenna array for LTE/WWAN and LTE MIMO operations," in *Proceedings of the 5th European conference on Antennas and Propagation (EUCAP)*, Rome, Italy, 2011, pp. 557-560.

[13] H. Li, Z. T. Miers, and B. K. Lau, "Design of orthogonal MIMO handset antennas based on characteristic mode manipulation at frequency bands below 1 GHz," *IEEE Transactions on Antennas and Propagation*, vol. 62, no. 5, pp. 2756−2766, 2014.

[14] R. G. Vaughan and J. B. Andersen, "Antenna diversity in mobile communications," *IEEE Transactions on Vehicular Technology*, vol. 36, no. 11, pp. 149−172, 1987.

Wonhee Lee

received his B.S. in IT engineering from Soonchunhayng University, Korea, in 2014. He is currently pursuing his M.S. in IT engineering at Soonchunhayng University, Korea. His current research interests include microwave circuit design and antennas.

Mingil Park

received his B.S. in IT engineering from Soonchunhayng University, Korea, in 2010 and his M.S. in IT engineering from Soonchunhayng University, Korea, in 2012. He is currently pursuing his Ph.D. in IT engineering at Soonchunhayng University, Korea. His research interests include antennas for the RF system, base station, and mobile phones.

Taeho Son

received B.S., M.S., and Ph.D. degrees from Hanyang University, Korea, in 1979, 1986, and 1990, respectively. From 1981–1982, he was a researcher with the Radar Center at Ferranti Co., Edinburgh, Scotland. He worked for Gold Star Precision Company as a team leader of the Radar and RF system Division from 1978 to 1987. Since 1990, he has been a professor in the Department of IT Engineering at Soonchunhyang University, Korea. He was a chairperson at the Korea Institute of Intelligent Transportation System in 2011. Moreover, he was a technical advisor at several companies concerned with the RF system and mobile phones, and he is working for advanced antenna engineering at Skycross Korea Company, Korea. Currently, his research is mainly focused on the design of various antennas for mobile communication and electronic systems for vehicles.